Available online at www.sciencedirect.com

SciVerse ScienceDirect

Journal of the European Ceramic Society 32 (2012) 1957–1964

www.elsevier.com/locate/jeurceramsoc

Densification of alumina by SPS and HP: A comparative study

Maryse Demuynck [a,*], Jean-Pierre Erauw [a], Omer Van der Biest [b], Francis Delannay [c], Francis Cambier [a]

[a] *Belgian Ceramic Research Centre (EMRA), Avenue Gouverneur Cornez 4, B-7000 Mons, Belgium*
[b] *MTM KULeuven, Kasteelpark Arenberg 44, B-3001 Leuven, Belgium*
[c] *EMPA UCLouvain, Place Sainte Barbe 2, B-1348 Louvain-la-Neuve, Belgium*

Received 15 July 2011; received in revised form 13 October 2011; accepted 18 October 2011
Available online 22 November 2011

Abstract

In this study, the densification of alumina by spark plasma sintering (SPS) was investigated and compared to conventional hot pressing. It was shown that SPS is very effective in the sintering of alumina leading to higher densities and allows to work at lower temperatures and with shorter sintering cycles. The effect of the heating rate is dependent on the heating mode (SPS or HP). The identification of active sintering mechanisms was attempted by an isothermal and an anisothermal methods, showing that other mechanisms probably related to electrical effects enhance the densification. We suggest the higher contribution of surface diffusion mainly during the initial stage of sintering and an influence of the presence of impurities segregated at the grain boundaries. They could create conductive layers and also introduce ions with a lower valence than Al^{3+}; defects are created in the surface layers and the diffusion of the species is increased.

Keywords: Spark plasma sintering (SPS); Hot pressing (HP); Al_2O_3; Sintering; Grain size

1. Introduction

In the field of sintered materials (ceramics, cermets, products from the powder metallurgy), performances are influenced by high densities, absence of defects, and by maintaining a microstructure as fine as possible. High density, defect free sintered materials can be obtained rather easily by hot pressing (HP) or hot isostatic pressing (HIP), but these techniques are perceived as expensive due to their discontinuous character and encapsulation technologies needed for the latter. Thereupon, as it is well known[1] that grain growth and densification kinetics are in competition (see Fig. 1), the ability to achieve fine microstructure in both of them is limited owing to the long processing time. Consequently, in a context where there is a need for densities close to theoretical density and microstructure as fine as possible, there is a great interest in fast sintering techniques such as spark plasma sintering (SPS).

In SPS, a high pulsed electric current flows through the graphite die and punches and through the powder when electrically conductive. The whole system is thus heated primarily by Joule effect. Such a technique enables reaching very high density while keeping a very fine microstructure in very short processing times (heating rates up to 1000 °C/min[2] and dwell times of only a few minutes). The low thermal inertia of the system and the absence of a massive insulation within the water cooled vessel, allow shortening the cooling step as well, thereby reducing significantly the overall thermal cycle. An additional advantage of the SPS is its applicability to a broad range of materials, including insulating powders. Using a nanometric α-alumina powder, Mishra and Mukherjee[3] obtained a relative density of 98% after 10 min at 1300 °C, a density level that was obtained by conventional sintering at 1500 °C after 3 h. The benefit of short processing cycle resulting from the high heating rates applicable in SPS was also demonstrated by Shen et al.[4] In their phenomenological parameter study, the effects of heating rate and applied load on the final density and grain size of a nanometric alumina were highlighted. In the temperature range of 1300–1400 °C, the heating rate was found to have no influence on the final density up to 300 °C/min. Higher heating rates however induced a slight decrease of density. In the same temperature range, the lower heating rate led to a more pronounced coarsening of the microstructure and to a larger average grain size.

* Corresponding author. Tel.: +32 65 40 34 73; fax: +32 65 40 34 60.
E-mail address: m.demuynck@bcrc.be (M. Demuynck).

0955-2219/$ – see front matter © 2011 Elsevier Ltd. All rights reserved.
doi:10.1016/j.jeurceramsoc.2011.10.031

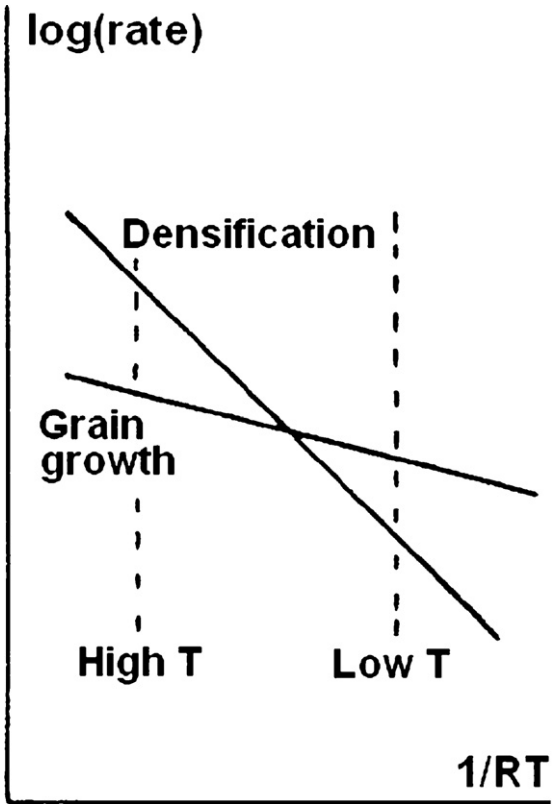

Fig. 1. Competition between densification rate and grain growth (from Ref. 1).

Despite the extensive use of SPS for the densification of poorly conductive oxide powders and of alumina in particular, the identification of the active sintering mechanism(s) and the potential contribution of athermal effects still appear as a pending issue and a debate subject. The assessment of the sintering mechanism was addressed only recently by Langer et al.[5] through a comparison between hot pressing and field-assisted sintering of two submicron alumina powders with different purity levels and average particle sizes. The experiments were performed at 1100–1250 °C with a dwell time between 1 and 2 h, a fixed heating rate of 10 °C/min and a macroscopic uniaxial pressure of between 15 and 50 MPa. It was shown that for both powders, the densification is enhanced in the case of field assisted sintering from the very beginning of the thermal cycle, this effect being more pronounced when considering the finest powder. It was concurrently demonstrated that the densification for both hot pressing and field assisted sintering proceeded by the same mechanism, namely grain boundary diffusion. However, it may be stressed that the heating rate used by these authors combined with the prolonged isothermal soaking times are not representative of sintering conditions usually used in SPS.

It was accordingly intended to investigate in the present study the influence of temperature, dwell time, heating rate and pressure on the overall densification process and resulting microstructure and to highlight the potential specific effect of applying an electrical field on the densification mechanism, when sintering submicron alumina at high heating rates (up to 250 °C/min) for short period of time (max. 6 min). To this end, as in the paper just cited, a direct comparison between SPS and hot pressing (under both resistive and inductive heating conditions) was carried out.

2. Experimental

A commercial alumina powder (P172SB, Alcan, France) was used as raw material. It has a purity of 99.7% (main impurities: 600 ppm Na_2O, 900 ppm SiO_2, 600 ppm CaO and 900 ppm MgO) and a mean particle size of 0.45 μm.

Three sintering methods were investigated. SPS experiments were carried out in an HPD25/1 equipment (FCT System, Germany) using a fixed pulse pattern of 10:5 ms on:off. Hot pressing experiments were performed, either under resistive heating conditions (KCE, Germany), or under inductive heating conditions (laboratory adapted induction furnace, UCLouvain, Belgium). These two hot pressing modes are further referred to in the text as HPR and HPI, respectively. Samples were sintered at 1300–1600 °C temperature range for 2–6 min under varying heating rates, the range of which depending on the sintering technique used: 10–250 °C/min in SPS, 20–100 °C/min in HPI and 2–10 °C/min in HPR, respectively. The tests were conducted under either constant or progressively increasing applied pressure as described elsewhere.[6] The samples sintered by SPS and HPI had a diameter of 20 mm; those sintered by HPR, a slightly larger diameter of 30 mm.

The density was measured using the Archimedes' water immersion method. Polished and thermally etched samples were observed by scanning electron microscopy (SEM, JEOL JSM-5900LV). The average grain size was determined by the linear intercept method according to the provisions of EN 623-3 (calculation on a minimum of 300 grains).

3. Results

3.1. Sintered density and microstructure

Whatever the sintering technique used, all samples reached full density, except those prepared at 1300 °C under the minimal load of 16 MPa. Accordingly, the final average grain size was taken as criterion to discriminate the potential influence of the investigated sintering parameters (maximum temperature, heating rate, dwell time, applied load). Fig. 2 shows the progressive coarsening of the microstructure with increasing maximum temperature and dwell duration, in samples sintered by SPS under 16–48 MPa at a heating rate of 200 °C/min. The effect of applied pressure and heating rate is illustrated in Fig. 3. Whereas the former leads to a marked coarsening above 32 MPa, the latter has no influence on the final microstructure. The density reached by the samples at the beginning of the dwell period is reported in Figs. 2 and 3 as well and shows similar trend, increasing with temperature, dwell time and applied pressure. Corresponding representative SEM micrographs are given in Fig. 4. MgO is usually used to inhibit grain growth but in non-optimized sintering conditions (like a too high temperature for example), an abnormal grain growth can be observed. The bimodal grain size distribution observed on Fig. 4 can be due to the impurities present in the powder inducing a preferential grain growth of

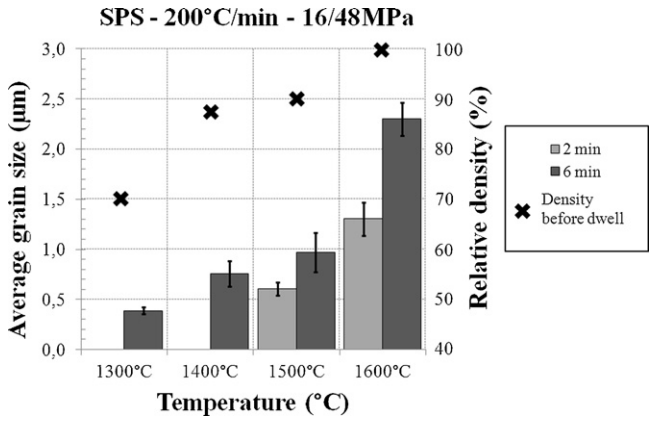

Fig. 2. Average grain size of SPS sintered alumina; effect of temperature and dwell time.

some particles. However, the standard deviation does not seem to increase with temperature or load and thus, the global grain coarsening observed (Figs. 2 and 3) concerns the whole grain population.

The effect of the heating rate on the average grain size was found to depend on the sintering technique used, as shown in Fig. 5. While an increase in heating rate has, as already said, no significant influence in SPS sintered samples, it leads to a decrease of grain size in HPR, and to grain coarsening in HPI.

A dependence on the sintering techniques was also observed for the densification behaviour at the lower temperature and heating rate ranges investigated. The density values of samples sintered by SPS, HPR and HPI for 6 min at 1300 °C under 16 MPa are shown in Fig. 6 for various heating rates ranging from 2 to 100 °C/min. Careful calibration tests were carried on the HPR and HPI equipments and the obtained results are very reproducible. However, SPS results are very sensitive to changes in some parameters (for example, after a calibration or modification of the tool design or graphite grade). Tests leading to the results shown in Fig. 6 are separated by several weeks and this could explain the dispersion observed. Another possible reason for this variation could be that the PID parameters of the SPS device are not optimized for regulating a test at the lower heating rate range. Despite the scatter only observed for the SPS data below 50 °C/min, the density reached by

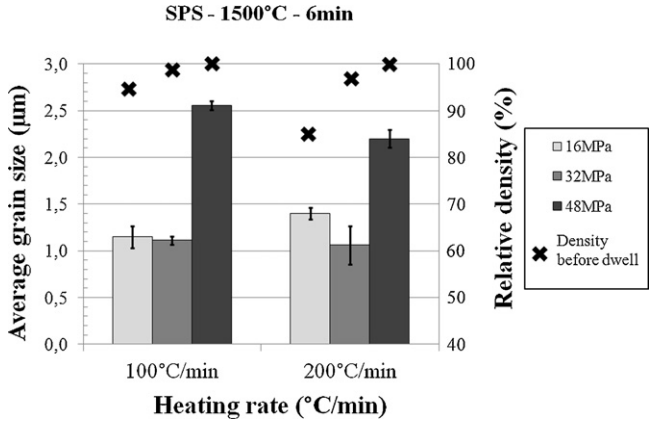

Fig. 3. Average grain size of SPS sintered alumina; effect of applied load.

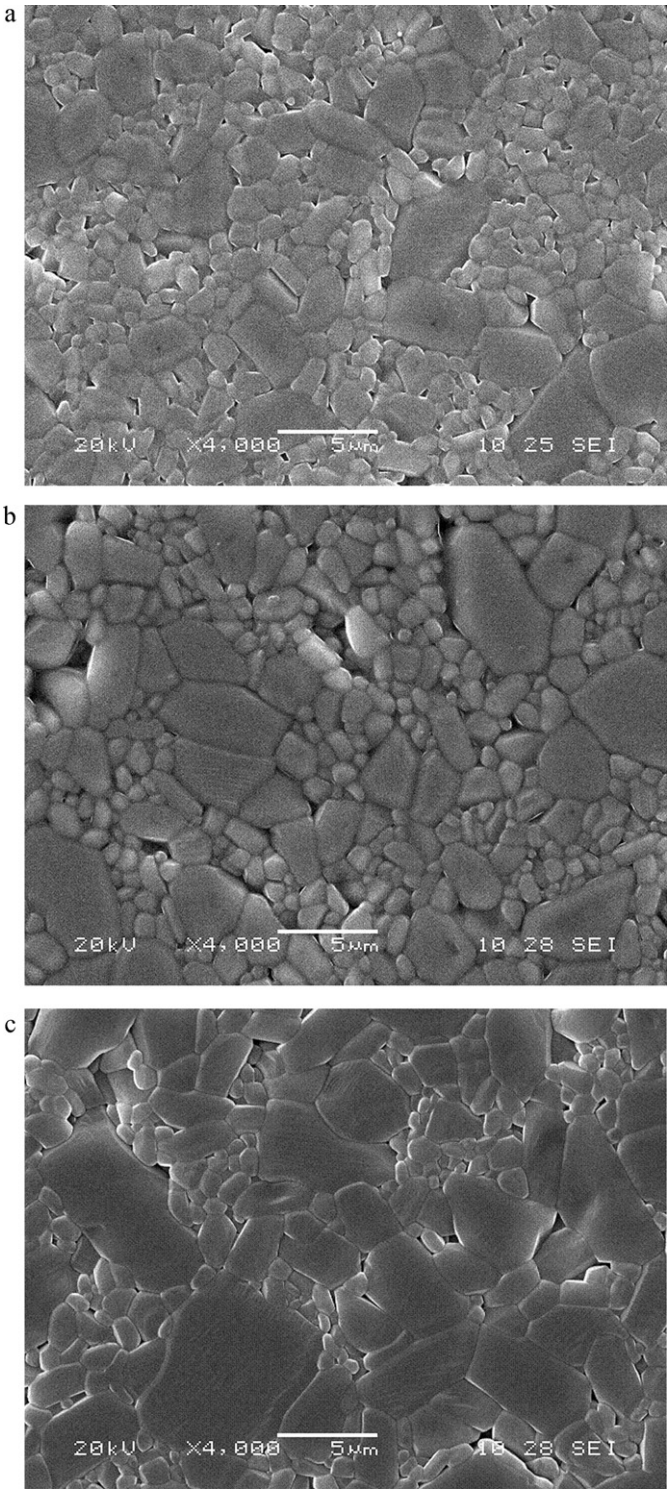

Fig. 4. SEM micrographs of samples sintered by SPS at 1500 °C for 6 min: (a) heating rate: 100 °C/min, applied load: 16 MPa; (b) heating rate: 200 °C/min, applied load: 16 MPa; (c) heating rate: 200 °C/min, applied load: 48 MPa.

SPS is significantly higher than that reached using either HPR or HPI, whatever the heating rate considered. It has been argued[7] that the more or less systematic lower densification temperatures reported in the literature for SPS could follow from an underestimation of the real sample temperature as a consequence of the specific temperature measurement position.

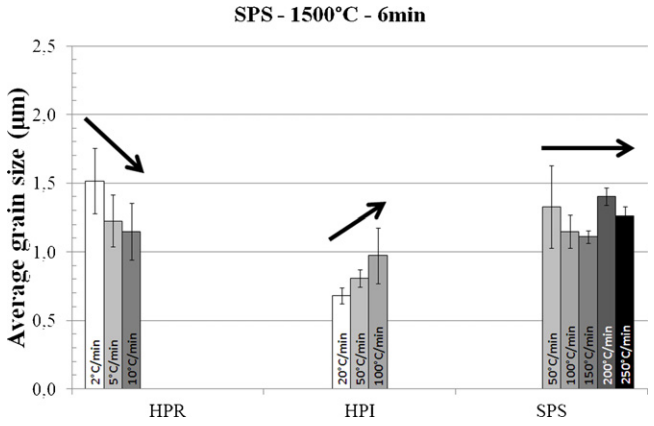

Fig. 5. Dependence of average grain size on heating rate and sintering technique (sintering temperature of 1500 °C and applied load 16 MPa).

It is true that in the present study, the temperature was measured in the SPS experiments at the bottom of the upper punch close to the sample surface whereas in both HPR and HPI, the temperature was measured radially at the surface of the graphite die. It cannot thus be excluded that a discrepancy in temperature reading partially contribute to the apparent lower densification of the HPR and HPI sintered alumina. In order to evaluate this contribution, dedicated SPS runs were performed under similar processing conditions but with simultaneous axial and radial pyrometer readings of the temperature. The details of these tests will be provided in a companion paper.[8] Fig. 7 shows the results obtained. On the non-conductive alumina, up to about 1450 °C, the outer surface of the graphite presents a higher temperature. At 1300 °C, the temperature difference between the two measuring locations amounts around 25 °C. It thus follows that the results of the HPR and HPI tests conducted at 1300 °C should be compared to SPS runs carried out at typically 1275 °C or inversely, that HPR and HPI tests should have been conducted at 1325 °C to allow an unbiased comparison with the 1300 °C SPS data. However, analysis of the SPS sintering

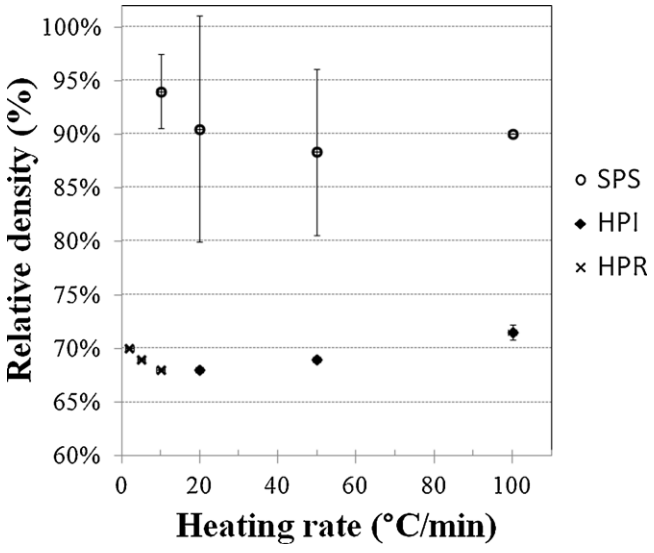

Fig. 6. Relative density values of samples sintered by SPS, HPI and HPR at 1300 °C for 6 min under 16 MPa using different heating rates.

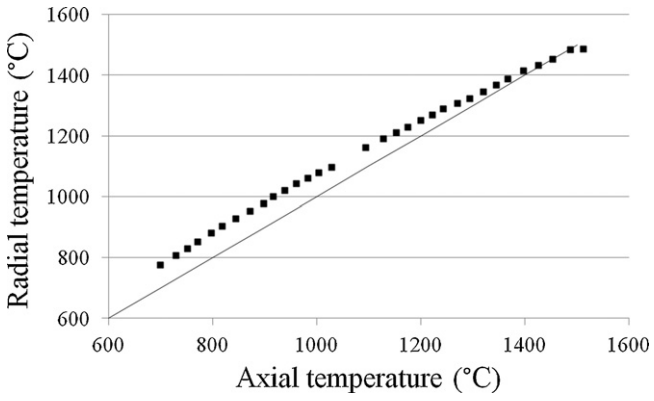

Fig. 7. Radial vs. axial temperature reading during a SPS run.

curves indicate that this 25 °C difference cannot on its own explain the large difference in final relative density observed here: despite some scatter in the results, density values in excess of 75–80% are already obtained in SPS sintered specimens at 1275 °C under moderate heating rates and without soaking time.

Fig. 8 shows that irrespective of the sintering technique used, the average grain size follows a unique sintering trajectory according to which, high density (of the order of 98%) can be reached before grain coarsening takes place. Similar behaviour has already be reported, both for zirconia[9] as for alumina.[5]

3.2. Densification kinetics and apparent activation energy

The densification mechanism involved during the SPS sintering of the alumina samples was investigated following two approaches.

The first one is identical to that adopted by Bernard-Granger and Guizard in their analysis of the densification by SPS of granulated zirconia.[9] Considering the densification process analogous to the high-temperature creep of a porous body, these authors suggested that the kinetic equation may be written as

$$\frac{1}{\rho}\frac{d\rho}{dt} = \frac{BD\mu_{eff}b}{kT}\left(\frac{b}{G}\right)^{p}\left(\frac{\sigma_{eff}}{\mu_{eff}}\right)^{n} \quad (1)$$

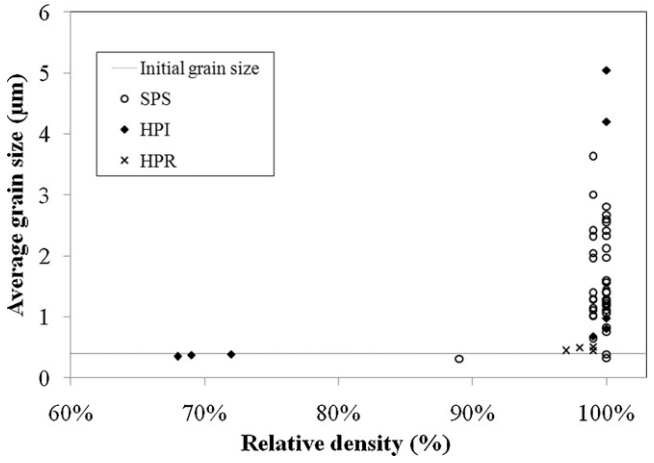

Fig. 8. Pooled sintering trajectory of SPS, HPI and HPR sintered samples.

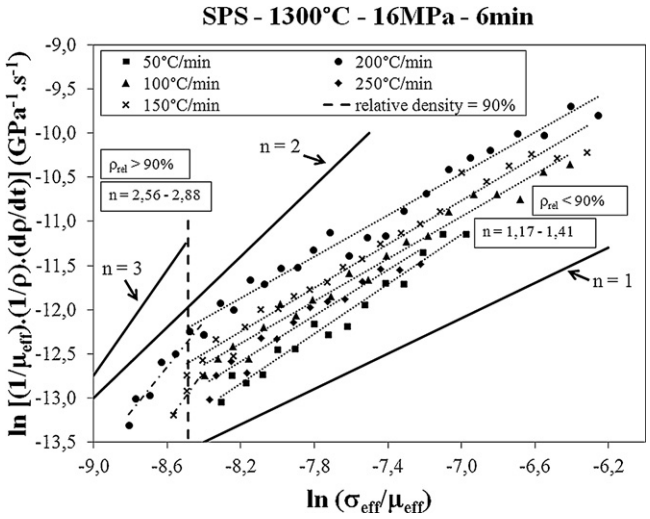

Fig. 9. Determination of the active sintering mechanism in the SPS densification of alumina; calculation of the stress exponent according to Eq. (3).

in which ρ is the instantaneous relative density, B a constant, D the diffusion coefficient, b the Burgers vector, k the Boltzmann's constant, T the absolute temperature, G the grain size, σ_{eff} the instantaneous effective stress acting on the porous body, μ_{eff} its instantaneous shear modulus, p and n, the grain size and stress exponent, respectively. Using appropriate expressions for the effective stress and effective shear modulus, the Eq. (1) can be reformulated as

$$\frac{1}{\mu_{eff}}\frac{1}{\rho}\frac{d\rho}{dt} = K\frac{\exp((-Q/RT))}{T}\left(\frac{b}{G}\right)^{p}\left(\frac{\sigma_{eff}}{\mu_{eff}}\right)^{n} \quad (2)$$

with K a constant and Q the apparent activation energy of the active densification mechanism. By taking the logarithm of both ends of Eq. (2), assuming constant grain size, constant temperature and constant apparent activation energy (i.e. a single densification mechanism active), the equation further transforms to

$$\ln\left(\frac{1}{\mu_{eff}}\frac{1}{\rho}\frac{d\rho}{dt}\right) = n\ \ln\left(\frac{\sigma_{eff}}{\mu_{eff}}\right) + K_1 \quad (3)$$

A plot of $\ln[(1/\mu_{eff})(1/\rho)(d\rho/dt)]$ as a function of $\ln(\sigma_{eff}/\mu_{eff})$ corresponding to the SPS experiments carried out at 1300 °C under 16 MPa for which the above hypotheses hold is shown in Fig. 9. The data points align along two groups of curves separated by a limit corresponding to a relative density of about 90%, corresponding roughly to closure of porosity. According to Eq. (3), the value of the stress exponent n can be obtained as the slope of the straight lines in Fig. 9. For relative densities below 90% (right part of Fig. 9) the stress exponent has a value around 1.3 (roughly between 1 and 2); for relative densities above 90% (left part of Fig. 9), n amounts to a higher value between 2 and 3 (around 2.7). A slight but marginal effect of the heating rate is observed as well.

The second approach is based on the analysis of the whole densification curves, including their anisothermal part, according to the formalism of the Master Sintering Curve (MSC) originally proposed by Su and Johnson.[10] The applicability of this approach to estimate the apparent activation energy and to foresee the extent of densification of alumina sintered by SPS has recently been demonstrated.[11] The method was extended here to the whole range of temperature and heating rate investigated. The results obtained by combining pairwise experiments carried out at a given temperature and successive heating rates are summarized in Table 1. For sintering tests at low heating rates (20–50 °C/min) in the 1300–1400 °C temperature range, the calculated apparent activation energy amounts 490–500 kJ/mol. In the same temperature range, increasing the heating rate to the typical level encountered for SPS (i.e. above 150 °C/min) leads to a decrease of the apparent activation energy to 320–350 kJ/mol. The estimated energy further drops as sintering temperature increases, reaching values as low as 140–160 kJ/mol for SPS runs at 1600 °C and heating rates above 150 °C/min.

4. Discussion

4.1. Grain growth

Whereas the influence of temperature, dwell time or applied load on the progressive coarsening of the microstructure are quite straightforward, the effect of heating rate (Fig. 5) and its dependence on the sintering technique appears less trivial. It can be shown however that this peculiar behaviour directly relates to the difference in sintering kinetics and the resulting difference of residence time at high temperature of dense samples (densities between 95 and 100%). This relative density range is selected as it was shown (Fig. 8) that grain growth occurs once the samples reached a density value in excess of typically 95%.

Fig. 10 shows the change of relative density in the range of 90–100% as a function of time for samples sintered for 6 min at 1500 °C. The time origin in Fig. 10 coincides with the beginning of the isothermal soaking period. In HPR (see Fig. 10a), with increasing heating rate, a density of 90% is clearly reached later (less than 10 min before dwell) and the residence time of the nearly dense sample at high temperature is shorter. Indeed, when it has reached a density higher than 90%, the sample sintered with an heating rate of 10 °C/min stays at high temperature for more or less 12 min while the sample sintered with an heating rate of 2 °C/min stays in these conditions for a much longer time of about 80 min. The die used in HPR is thicker than those used in HPI and SPS and is heated by an external resistance. So it needs time for the heat to progress inwards from the outer rim of the die to the sample. As a consequence, the higher the heating rate, the colder the sample in the centre of the die and the smaller the final grain size. In HPI (Fig. 10b), the density level of 90% is reached during the isothermal stage and the heating rate further affects the densification with time. The sample heated at 100 °C/min reaches the full density after 1 min dwell while the sample heated at 20 °C/min does not reach the maximum density after 6 min. The higher the heating rate used to reach the dwell temperature, the shorter the time to reach full density and thus, the longer the period for grain growth. Accordingly, as observed, the average grain size increases with increasing heating rate. Finally, in SPS (Fig. 10c), despite a significant influence of the heating rate

Table 1
Apparent activation energies calculated according to the MSC method.

T (°C)	Heating rate (°C/min)					
	20	50	100	150	200	250
1300	502 kJ/mol		322 kJ/mol	319 kJ/mol	350 kJ/mol	
1400	489 kJ/mol					
1500		306 kJ/mol	218 kJ/mol	160 kJ/mol	224 kJ/mol	
1600			163 kJ/mol	140 kJ/mol		

on the densification progress during heating and on the density reached at the onset of the dwell (higher temperature gradients with higher heating rates), this density rapidly evolves to its maximum level in the first seconds of the isothermal soaking period (all the samples reach the maximum density nearly at the same time). It follows that whatever the heating rate, the residence time at high temperature of all samples with density in excess of 95% is practically identical which explains the absence of significant dependence of average grain size on heating rate in this case. However, if the maximum density is reached before the beginning of the dwell, the higher the heating rate, the smaller the grain size because in that case the maximum density is reached later with a faster temperature ramp. An advantage of SPS is thus to give the possibility to work with higher heating rates and lower temperatures.

4.2. Sintering mechanism

The investigation of the densification mechanism(s) active in the SPS sintering of alumina by a classical isothermal method could only be performed using the 1300 °C data. For higher sintering temperatures, the major part, if not the whole part, of the densification takes place during the heating portion of the thermal cycle, i.e. under anisothermal conditions. Only the stress exponent n, could accordingly be derived. The obtained value, depending on the heating rate considered, lies in the range of 1.2–1.4 for relative densities up to 90% and amounts about 2.7 above. A n value of 1 corresponds to either grain boundary diffusion, lattice diffusion or viscous flow, the first mechanism being the most often invoked in the literature for explaining the densification of pure submicron alumina powder.[12] The value of the apparent activation energy calculated from the sintering runs carried out at this same temperature under moderate heating rate (20–50 °C/min) by the anisothermal MSC approach, $Q \approx 500$ kJ/mol, supports as well the idea that the densification in this temperature and heating rate range occurs primarily by grain boundary diffusion.[10,12] However, the significantly higher density values obtained by SPS at this temperature with respect to the hot pressing techniques (both resistive and inductive) as well as the surprisingly low apparent activation energy values estimated for higher temperatures and/or heating rates strongly suggest that additional densification mechanisms might be involved.

This improved densification most probably results from the peculiar heating mode in SPS that potentially induces athermal effects related to the presence of an electrical field. The presence of an electrical field can potentially affect surface phenomena by modifying the grain boundary energy and interface kinetics.[13] This could lead to a delay in the grain growth process and a resulting enhanced sinterability. Even in poorly conducting materials like alumina, the presence of an electric field has been shown to drastically enhance the diffusion of species contributing to densification[14] (change in the rate-controlling diffusion mechanism). Very recently, it has been demonstrated that an adequate combination of electrical field and temperature could lead to a quasi instantaneous densification of ion conductive material like zirconia[15] as well as of other material like MgO-doped alumina.[16] Finally we have to keep in mind that despite its insulating character at room temperature, alumina becomes conductive at high temperature.[17] Its resistivity is indeed

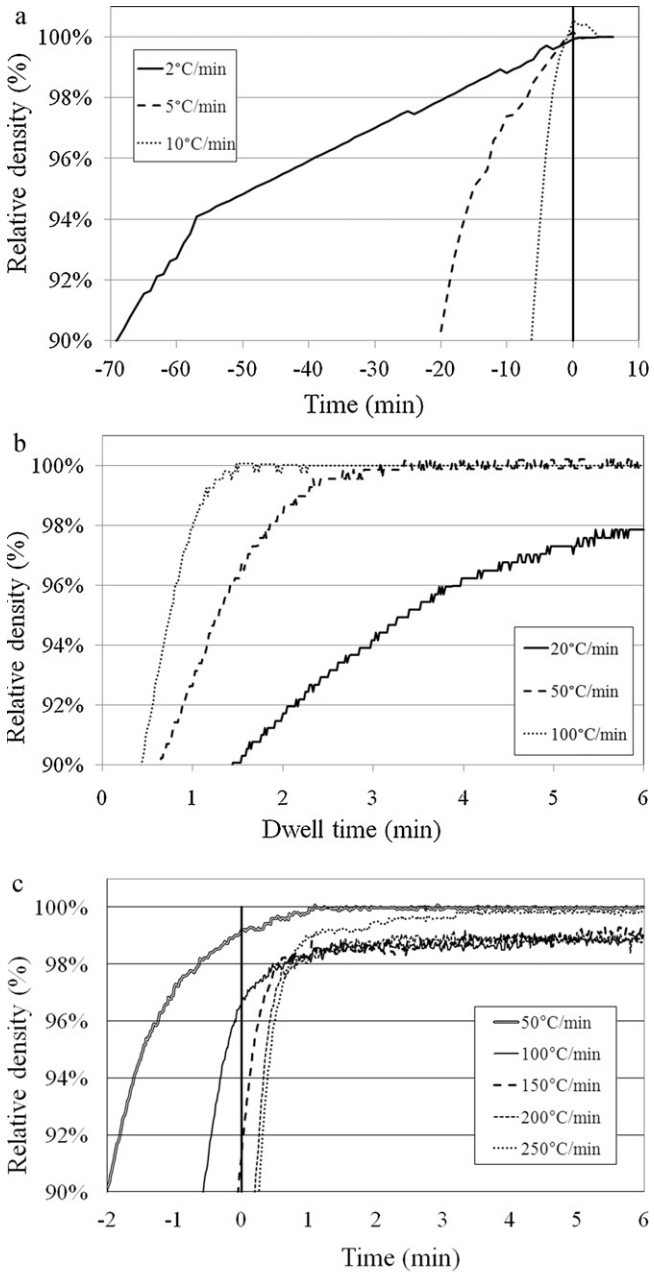

Fig. 10. Change of relative density with time during soaking at 1500 °C for 6 min under 16 MPa: (a) HPR sintering run; (b) HPI sintering run; (c) SPS sintering run.

influenced by the purity level but even for low impurity content, a higher surface conductivity can result from the application of an external electrical field and small surface currents can consequently appear. They are probably not sufficient to induce a Joule effect[18] but they were assumed to favour the formation of sintering necks at an early stage of densification.[19,20]

5. Conclusion

It has been shown in this study that SPS is a very efficient technique for the densification of an insulating material like Al_2O_3. A scatter in the SPS results was observed at the lower end of the temperature range investigated (1300 °C), stressing the difficulty to reach a good reproducibility of the results in the lower heating rate range and the relative importance of some changes (graphite grade, design of the tool, calibration, etc.) to the obtained results. However in all experiments, higher alumina densities were reached than in classical hot pressing with the same processing parameters.

To approach the densification mechanisms, two different methods were used. A classical approach to determine the n values using isothermal data could only be applied at 1300 °C, because full density is reached during an isothermal treatment. It was shown that two different values are obtained, whatever the used heating rate: n between 1 and 2 for densities less than 90% and n between 2 and 3 for higher densities, leading to the conclusion that grain boundary diffusion cannot be the sole densification mechanism. The surface diffusion is probably enhanced from the very beginning of the sintering cycle leading to a faster formation of the sintering necks during the initial stage of sintering. The high heating rates applied in SPS allow reaching quickly a temperature range where the densification process is favoured and kinetically separated from grain growth. The impurities could also play an important role. As tests were carried out on a commercial powder with 0.3% of impurities, it is likely to consider that those impurities could be mainly segregated at grain boundaries leading to the presence of conductive layers. The impurities also introduce ions with a lower valence than Al^{3+} in the system and create defects in the surface layers. As a consequence of high currents applied during SPS, a softening of the surface layers is possible leading either to a grain rearrangement by sliding under the applied load or to an enhanced migration of species through the surface layer.

Using the Master Sintering Curve formalism, apparent activation energies were calculated for the full range of data. Values around 490 kJ/mol, typical of densification by grain boundary diffusion, were only found at lower temperature and lower heating rates. Much lower apparent activation energy values were found for higher sintering temperatures and heating rates, suggesting the contribution of additional mechanisms most probably related to the presence of the electric field and to the increasing electrical conductivity of the samples at high temperature.

Acknowledgements

M. Demuynck would like to thank the DGO6 (Wallonia, Belgium) for the financial support of her PhD thesis under contract no. 616389.

References

1. Harmer MP, Brook RJ. Fast firing – microstructural benefits. *J Br Ceram Soc* 1981;**80**:147.
2. Munir ZA, Anselmi-Tamburini U, Ohyanagi M. The effect of electric field and pressure on the synthesis and consolidation of materials: a review of the spark plasma sintering method. *J Mater Sci* 2006;**41**:763–77.
3. Mishra RS, Mukherjee AK. Electric pulse assisted rapid consolidation of ultrafine alumina matrix composites. *Mater Sci Eng* 2000;**A287**:178–82.

4. Shen Z, Johnsson M, Zhao Z, Nygren M. Spark plasma sintering of alumina. *J Am Ceram Soc* 2002;**85**(8):1921–7.
5. Langer J, Hoffmann MJ, Guillon O. Direct comparison between hot pressing and electric field-assisted sintering of submicron alumina. *Acta Mater* 2009;**57**:5454–65.
6. Demuynck M, Erauw JP, Van der Biest O, Delannay F, Cambier F. Densification de l'alumine et de composites à base d'alumine ou de nitrure d'aluminium par FAST et pressage uniaxial à chaud conventionnel: Etude comparative. In: *Proceedings of Colloque Poudres et Matériaux Frittés*. 2011.
7. Langer J, Quach DV, Groza JR, Guillon O. A comparison between FAST and SPS apparatuses based on the sintering of oxide ceramics. *Int J Appl Ceram Technol* 2011;**8**(6):1459–67.
8. Demuynck M, Erauw JP, Van der Biest O, Delannay F, Cambier F. Densification of Al_2O_3–TiC and AlN–TiC composites by FAST: the effect of the transport properties, in preparation.
9. Bernard-Granger G, Guizard C. Spark plasma sintering of a commercially available granulated zirconia powder: I. Sintering path and hypotheses about the mechanism(s) controlling densification. *Acta Mater* 2007;**55**:3493–504.
10. Su H, Johnson DL. Master sintering curve: a practical approach to sintering. *J Am Ceram Soc* 1996;**79**(12):3211–7.
11. Erauw JP, Demuynck M, Cambier F, Vanmeensel K, Van der Biest O. Applicability of the master sintering curve concept to spark plasma sintering. In: *MS&T'10 Conference Proceedings*. 2010. p. 2288–99.
12. Wang J, Raj R. Activation energy for the sintering of two-phase alumina/zirconia ceramics. *J Am Ceram Soc* 1991;**74**(8):1959–63.
13. Ghosh S, Chokshi AH, Lee P, Raj R. A huge effect of weak dc electrical fields on grain growth in zirconia. *J Am Ceram Soc* 2009;**92**(8):1856–9.
14. Yang D, Conrad H. Plastic deformation of fine-grained Al_2O_3 in the presence of an electric field. *Scr Mater* 1999;**41**(4):397–401.
15. Cologna M, Rashkova B, Raj R. Flash sintering of nanograin zirconia in <5 s at 850 °C. *J Am Ceram Soc* 2010;**93**(11):3556–9.
16. Raj R. Influence of applied DC electrical field on sinterforging experiments with oxides. In: *Oral communication, materials science & technology 2010 conference and exhibition*. 2010.
17. Morrell R. *Handbook of properties of technical and engineering ceramics. Part 2: data reviews. Section I: high alumina ceramics*. London: Her Majesty's Stationary Office; 1987, 255 p.
18. Carney CM, Mah TI. Current isolation in spark plasma sintering of conductive and nonconductive ceramics. *J Am Ceram Soc* 2008;**91**(10):3448–50.
19. Munir ZA, Quach DV, Ohyanagi M. Electric current activation of sintering: a review of the pulsed electric current sintering process. *J Am Ceram Soc* 2011;**91**(1):1–19.
20. Stanciu L, Quach D, Faconti C, Groza JR, Raether F. Initial stages of sintering of alumina by thermo-optical measurements. *J Am Ceram Soc* 2007;**90**(9):2716–22.